Journal of Photochemistry and Photobiology A: Chemistry 198 (2008) 60–68

Contents lists available at ScienceDirect

Journal of Photochemistry and Photobiology A: Chemistry

journal homepage: www.elsevier.com/locate/jphotochem

Photoreaction and photopolymerization studies on fluoflavin dye–pyridinium salt systems

Radosław Podsiadły*

Institute of Polymer and Dye Technology, Technical University of Lodz, Stefanowskiego 12/16, 90-924 Lodz, Poland

ARTICLE INFO

Article history:
Received 23 January 2008
Received in revised form 13 February 2008
Accepted 21 February 2008
Available online 4 March 2008

Keywords:
Fluoflavin dyes
Photoinitiator
Alkoxypyridinium photodecomposition
Photopolymerization
Photoinduced electron transfer

ABSTRACT

Several dyes derived from 5,12-dihydroquinoxalino[2,3b]quinoxaline have been synthesised and evaluated as sensitizers for alkoxypyridinium salt photodecomposition. The results are discussed on the basis of the free energy change for electron transfer from fluoflavin dyes to alkoxypyridinium compounds. The mechanism of dye photobleaching is supported by DFT calculations, spectroscopic characterization of the cation radical of the dye, and the quantum yields of sensitised proton formation. Fluoflavin dyes are shown to be useful as photoinitiators for sensitizing compounds to photooxidation. Photoredox pairs consisting of fluoflavin dyes and alkoxypyridinium salt are found to be effective initiation systems for free radical polymerization of methyl acrylate and trimethylolpropane triacrylate (TMPTA) using VIS light.

1. Introduction

One of the most widely used and simplest methods of polymer formation is radical-chain addition polymerization. Light-induced photopolymerization has several advantages over other methods. The process involves low temperatures, and it can be controlled by manipulating the intensity and wavelength of irradiation. Photoinitiated free radical polymerization of multifunctional monomers produces highly crosslinked polymers with high thermal stability, mechanical strength, and resistance to solvent. These polymers have many industrial applications, especially in coatings for flooring and furniture, dental restorative materials, optical fibre coatings, hard and soft contact lenses, and photolithography [1].

Many early photoinitiating systems were sensitive to UV light but a large number of systems have since been developed that extend the spectral sensitivity to the visible range. In the early photoinitiators, the direct photofragmentation process in the excited state yields free radicals, as shown in Scheme 1 for benzoin aryl ether [2]. The latter process is a panchromatic sensitization, which requires the presence of a suitable dye as primary absorber [3–8]. In this case the processes following photoinduced intermolecular electron transfer (PET) yield free radicals that initiate polymerization. Two different types of dye sensitization may be considered. The first type is the photoreducible sensitization (Scheme 2) in which the dye (xantene, acridine, and cyanine) is photoreduced in the presence of a suitable reductant (*N*-phenylglycine [3], phenylthioacetic acid [4], alkyltriphenylborane [5]). The second type is the photooxidation of the dye by a strong electron acceptor, e.g. alkoxypirydynium salt (Scheme 3) [6]. This type of sensitisation is used much less often. The reason is at least partly because of the limitations of this approach: only cyanine [6], ketocoumarin [7] and acridinedione dyes [8] initiate acrylate monomer photopolymerization via electron transfer from the excited states of the dyes to onium salts.

Initiator systems working in the visible range are used in pigmented coatings, sunlight curing of waterborne latex paints, curing of inks, and high-speed laser imaging [9].

The main goal of this study is the synthesis of fluoflavin dyes (**1**–**5**) and the evaluation of their spectroscopic and electrochemical properties. This paper also reports the photochemical properties of pyridinium (**Py1**-**Py2**)/fluoflavin dye systems. In particular, the photobleaching of fluoflavin dye and the sensitised decomposition of pyridinium salt (**Py1**) are discussed. The mechanism of dye fading proposed here is supported by density functional theory (DFT) calculations, spectroscopic characterization of their cation radicals and the quantum yields of sensitised proton formation. Finally, the study demonstrates that these new photooxidizable sensitization systems can be used as visible photoinitiators for free radical polymerization of acrylate monomers.

* Fax: +48 42 636 25 96.
E-mail address: radekpod@p.lodz.pl.

1010-6030/$ – see front matter © 2008 Elsevier B.V. All rights reserved.
doi:10.1016/j.jphotochem.2008.02.016

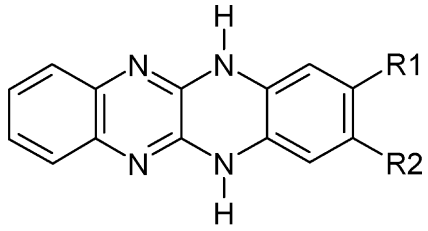

Dye	R1	R2
1	H	H
2	H	Br
3	H	Cl
4	H	Me
5	Me	Me

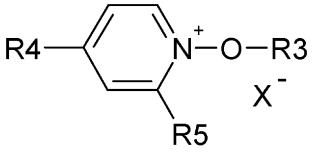

	R3	R4	R5	X
Py1	Me	Ph	H	BF_4
Py2	Et	H	Me	PF_6

2. Experimental

2.1. General

Synthesis reagents and **Py1** were purchased from Aldrich (Poznan, Poland) and POCh (Gliwice, Poland). The final products were identified by ^{1}H NMR spectroscopy [Bruker Avance DPX 250, DMSO-d_6, TMS, δ (ppm)]. Their purity was also checked through TLC

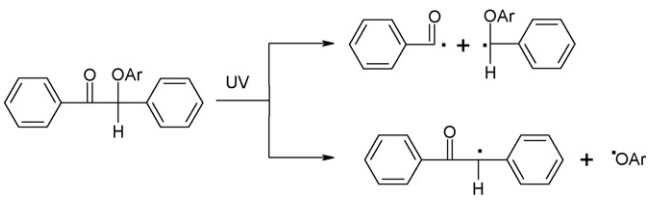

Scheme 1.

[Merck Silica gel 60 solvent toluene: butyl acetate 5:1 (v/v)]. The absorption and steady-state fluorescence spectra were recorded using a Lambda 40 spectrophotometer (PerkinElmer) and a FluoroLog 3 spectrofluorimeter (Jobin Yvon-Spex), respectively.

2.2. Synthesis

2.2.1. Synthesis of 2,3-dimethyl-5,12-dihydroquinoxalino[2,3b]quinoxaline [10]

2,3-Dichloroquinoxaline (1.99 g, 0.01 mol) and 4,5-dimethyl-*o*-phenylenediamine (2.72 g, 0.02 mol) were refluxed in ethylene glycol (20 ml) for 0.5 h. After cooling, the orange precipitate was filtered, washed with methanol, dried, and recrystallised from acetic acid. The product (2.33 g) was obtained in 88% yield. The other dyes were synthesised in the same way using the appropriate *o*-phenylenediamines. ^{1}H NMR data for all dyes are presented in Table 1.

2.2.2. Synthesis of N-ethoxy-2-methylpiridinium hexafluorophosphate [11]

2-Methylpyridine *N*-oxide (1.09 g, 0.01 mol) and triethyloxonium hexafluorophosphate (2.98 g, 0.012 mol) were refluxed in chloroform (3 ml) for 0.5 h. The crystalline product was recrystallised twice from an ethanolic solution.

m.p. 89 °C; ^{1}H NMR: 1.50 t (J = 7.00, 3H), 2.85 s (3H), 4.62 q (J = 7.00, 2H), 7.91–8.01 m (2H), 8.38 dt (J_1 = 1.25, J_2 = 6.50, 1H), 9.00 dd (J_1 = 1.25, J_2 = 6.50, 1H).

2.3. Photochemical experiments

All photochemical experiments were carried out in a Rayonet Reactor RPR 200 (The Southern New England Ultraviolet Co.) equipped with eight lamps emitting light at 419 nm. Illumination intensity was measured using uranyl oxalate actinometry [12].

Photodecomposition of **Py1** (1 mM) sensitised by fluoflavin dye (0.1 mM) in 1-methyl-2-pyrrolidone (5 ml) was carried out in a glass tube under an N_2 atmosphere. The decomposition of methoxypyridinium salt was monitored spectrophotometrically after dilution with 1-methyl-2-pyrrolidone (1:1, v/v). The extent of dye fading was determined according to the decrease in absorption at λ_{max}.

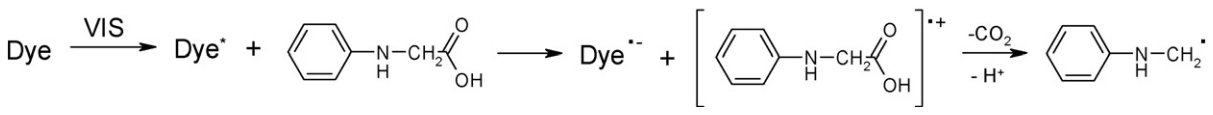

Scheme 2.

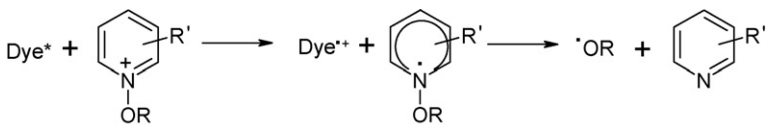

Scheme 3.

Table 1
Yield, ^{1}H NMR spectra and R_f of dyes **1**–**5**

Dye[a]	Yield (%)	^{1}H NMR [DMSO-d_6, TMS int. (ppm)]	R_f[b]
1	70	0.16 bs (2H), 6.51–7.36 m (8H)	0.61
2	30	6.76–6.95 m (7H), 7.94 bs (2H)	0.46
3	46	6.62–6.97 m (7H), 10.07 bs (2H)	0.49
4	60	2.17 s (3H), 6.34–7.35 m (7H), 9.84 bs (2H)	0.59
5	88	1.94 s (6H), 6.56–6.76 m (4H), 7.42 s (2H), 8.51 bs (2H)	0.20

[a] m.p. > 360 °C.
[b] Merck Silica Gel 60; toluene butyl acetate 5:1 (v/v).

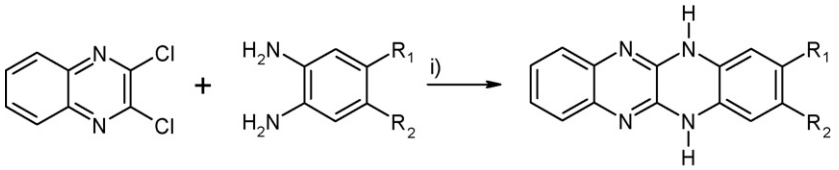

Scheme 4. (i) Ethylene glycol, reflux 0.5 h.

The quantum yield of dye bleaching Φ_{bl} was calculated from at least three determinations when the reaction was 14 ± 3% complete.

The quantum yield of sensitised proton formation $\Phi(H^+)$ was determined using sodium bromophenol blue (**BPhBl**). The proton concentration was estimated from the calibration of optical density of **BPhBl** vs. water-free hexafluoroantimonic acid. The $\Phi(H^+)$ was calculated from at least three determinations when the reaction was 14 ± 3% complete.

The quantum yield of singlet oxygen formation Φ ($^1O_2$) was determined from the ratio of the rates of the dye-induced disappearance of tetraphenylcyclopentadienone (TPC) and the rates of the perinaphthenone-induced disappearance of TPC, using its known quantum yield of triplet formation $\Phi_T = 0.95$ [13].

The fluorescence quantum yield of the dye (Φ_{dye}) was calculated from the following equation:

$$\Phi_{dye} = \frac{\Phi_{ref} I_{dye} A_{ref} n_{dye}^2}{I_{ref} A_{dye} n_{ref}^2} \quad (1)$$

where Φ_{ref} denotes the fluorescence quantum yield of the Rhodamine 101 reference ($\Phi_{ref} = 1.0$ in ethanol [14]), A_{dye} and A_{ref} denote the absorbance of the dye and the reference at their excitation wavelengths, I_{dye} and I_{ref} refer to the areas under the fluorescence peaks for the dye and reference, and n_{dye} and n_{ref} are the solvent refractive index for the dye and the reference, respectively.

The Stern–Volmer constants were obtained from fluorescence quenching experiments. The fluorescence spectra of dye solutions (4–6 μM) in 1-methyl-2-pyrrolidone containing various amounts of quenchers were measured at room temperature in an air atmosphere using excitation at 440 nm or 400 nm for **Py1** or **Py2**, respectively. Relative fluorescence intensities (I_0/I) were determined by measuring the heights of the peak at λ_{em}.

Fluorescence lifetime measurements were made using time-correlated single photon counting (Edinburgh Analytical Instruments Co.). The light source was a hydrogen lamp of thyratron with a frequency of 40 kHz. The excitation and emission bandpasses were 3.6 nm. The instrument response function was recorded by collecting scattered light from a Ludox silica suspension. Fluorescence decay from both sample and scattering solution was acquired to the level of 1.0×10^4 counts at the peak. Fluorescence decays were fitted to a sum of exponentials (Eq. (2)):

$$I(t) = \sum_i^n \alpha_i \exp(-t/\tau_i) \quad (2)$$

with amplitudes α_i and decay lifetimes τ_i. The average lifetimes $\langle\tau\rangle$ for biexponential decays of fluorescence were calculated from the decay times and preexponential factors using the following equation:

$$\langle\tau\rangle = \frac{\sum \alpha_i \tau_i^2}{\sum \alpha_i \tau_i} \quad (3)$$

Photopolymerization was carried out in solutions composed of 1 ml of 1-methyl-2-pyrrolidone and 4 ml of methyl acrylate or trimethylolpropane triacrylate (TMPTA). Dye concentration was 0.1 mM, and the concentration of alkoxypyridinium salts was 10 mM. The rate of polymerization (R_p) was calculated using Eq. (4) where Q_s is heat flow per second during reaction, m is the mass of the monomer in the sample, M is the molar mass of the monomer, n is the number of double bond per monomer, and ΔH_p is the theoretical enthalpy for complete conversion of acrylate double bonds (20.6 kcal/mol) [15].

$$R_p = \frac{Q_s M}{n \Delta H_p m} \quad (4)$$

For the detection of the heat flow, a PT 401 temperature sensor (Elmetron) immersed in the sample was used.

Table 2
Spectroscopic[a], photophysical[a], and electrochemical[b] parameters of fluoflavin dyes

Dye	λ_{max} (nm)	lg ε_{max}	λ_{em} (nm)	Φ_{fl}	Singlet lifetime (ns)	SS (nm)	$E(S^*)$ (kJ mol^{-1})	$\Phi(^1O_2)$	$E^{ox}_{1/2}$ (V)
1	417	4.23	485	0.80	4.23	68	267	0.08	0.21
2	419	4.18	491	0.37	3.31	72	264	0.65	0.24
3	419	4.19	489	0.60	3.53	70	266	0.25	0.25
4	420	4.16	490	0.82	4.17	70	264	0.06	0.17
5	422	3.97	490	0.60	4.12	68	264	0.05	0.16

[a] In 1-methyl-2-pyrrolidone.
[b] In DMF.

The conversion of methyl acrylate into poly(methyl acrylate) after a 2-min irradiation was determined gravimetrically.

2.4. Electrochemical experiments

The electrochemical experiments were carried out in dimethylformamide (DMF) solutions containing 0.1 M tetra-*n*-butylammonium perchlorate as supporting electrolyte. All experiments were carried out at room temperature and solutions were degassed prior to experiments by bubbling with argon. During each experiment, a blanket of argon was maintained over the solution. The concentration of the dyes and pyridinium salt was 1 mM. Cyclic voltammograms were recorded on an AUTOLAB potentiostat (Ecochemie, Holland). Platinum was used as both the working and auxiliary electrodes and ferrocene was used as the reference electrode [16].

2.5. Quantum chemical calculations

The geometries of all species were optimised by the B3LYP density functional method [17,18] as implemented in the Gaussian 98 suite of programs [19]. The above calculations were performed for the ground states using standard 6-31G* basis set. The optimised structures were characterized by harmonic frequency analysis as local minima (all frequencies real). The zero point vibrational energy and enthalpy correction were used without scaling.

3. Results and discussion

3.1. Synthesis, spectroscopic, and electrochemical characterization of fluoflavin dyes

It is well known from the literature that the fluoflavins can be obtained by heating *o*-phenylenediamine with 2,3-dichloroquinoxaline in a melt [20] or in the presence of solvents such as DMF [21] or ethylene glycol [10]. In the former case the main product is contaminated with 1H,1′H-[2,2′]bis(benzimidazolyl). In the present study the fluoflavin dyes were synthesised by heating the appropriate substrates in ethylene glycol according to the Scheme 4. The crude dyes were purified by recrystallization from acetic acid until a constant molar excitation coefficient and TLC purity were obtained.

The chemical structure of the dyes was verified by ^{1}H NMR (Table 1). The spectroscopic properties (absorption and fluorescence) of dyes **1**–**5** are presented in Table 2. Dyes **1**–**5** have an absorption band in the visible region located at approximately 420 nm and a strong emission band characterized by a Stokes shift of ~68–70 nm. The electronic absorption and emission spectra of dye **1** across the UV–vis range are presented in Fig. 1. The absorption spectra are typical of policyclic aromatic heterocycles, which have a characteristic vibrational structure. For all dyes tested, the absorption and fluorescence spectra are almost mirror images of each other with overlapping bands corresponding to the $0 \rightarrow 0$ transition. The fluorescence quantum yield and the lifetime of the singlet excited state are presented in Table 2. As can be seen from these data the fluorescence quantum yield of these dyes is in the range of 0.37–0.80, and the singlet lifetime is in the range of 3.31–4.23 ns. Dye **2** exhibits the smallest values for both parameters.

The electrochemical experiments were carried out in DMF. The cyclic voltammogram of dye **1** is presented in Fig. 2, and the detailed results of the electrochemical experiments are presented in Table 2. In all cases the electrochemical oxidation was irreversible and the location of the oxidation peak depended on the structure of the dye. The results indicate that the dyes **4** and **5** are more readily oxidised then the halogen-substituted analogues **2** and **3**. This is illustrated by the position of the oxidation peak at 0.17 V and 0.16 V for dyes **4** and **5** and at 0.24 V and 0.25 V for dyes **2** and **3**, respectively.

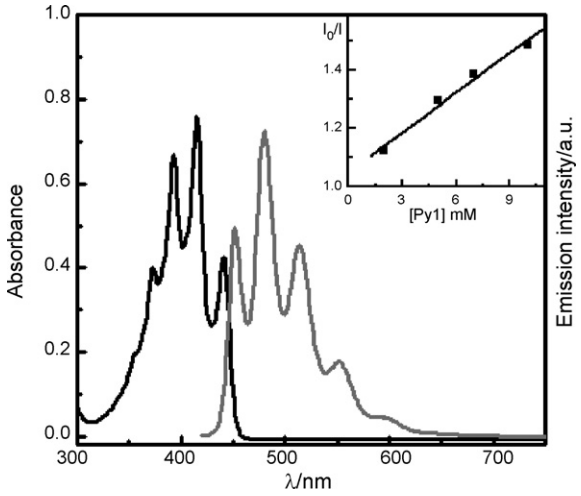

Fig. 1. Normalized absorption (black) and emission (gray) spectra of dye **1** (30 μM) in 1-methyl-2-pyrrolidone. *Inset*: Stern–Volmer plot of fluorescence quenching of dye **1** (4 μM) by **Py2** in 1-methyl-2-pyrrolidone.

3.2. Photodecomposition of Py1-sensitised fluoflavin dyes

The well-known mechanism [6] of dye-sensitised photodecomposition of alkoxypyridinium salt (Py) is presented in Scheme 3. Irradiation of this photoredox pair leads to electron transfer from the excited sensitizer (Dye^*) to Py, followed by cleavage of the alkoxypiridinium radical ($Py^\bullet$) to give alkoxy radical ($^\bullet OR$), neutral pyridine, and sensitizer radical cation ($Dye^{\bullet+}$).

Dyes **1**–**5** were evaluated for their efficacy as sensitizers for **Py1** photodecomposition. The process was studied in 1-methyl-2-pyrrolidone under an N_2 atmosphere, and the decomposition of **Py1** was monitored spectrophotometrically at 350 nm. The absorption spectra of the dye **4**/**Py1** combination before and during irradiation are shown in Fig. 3. During irradiation for 10–30 s the absorption of both **Py1** and dye **4** decreased (Fig. 3A and B, respectively). The same behaviour was also observed for other dye/**Py1** combinations.

The calculated relative rate of **Py1** decomposition ($v_{dec}^{rel} = v_{dec}dye/v_{dec}dye$ **1**) is presented in Table 3. The results show that dye **2** is the most effective sensitizer for decomposition of **Py1**.

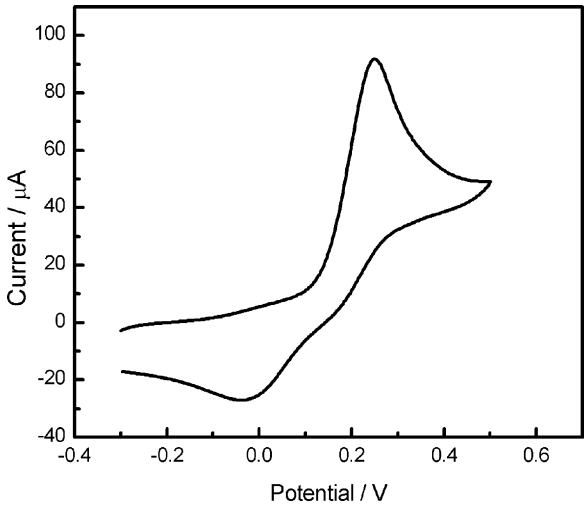

Fig. 2. Cyclic voltammograms of dye **1** in DMF. Scan rate: 0.1 V s^{-1}.

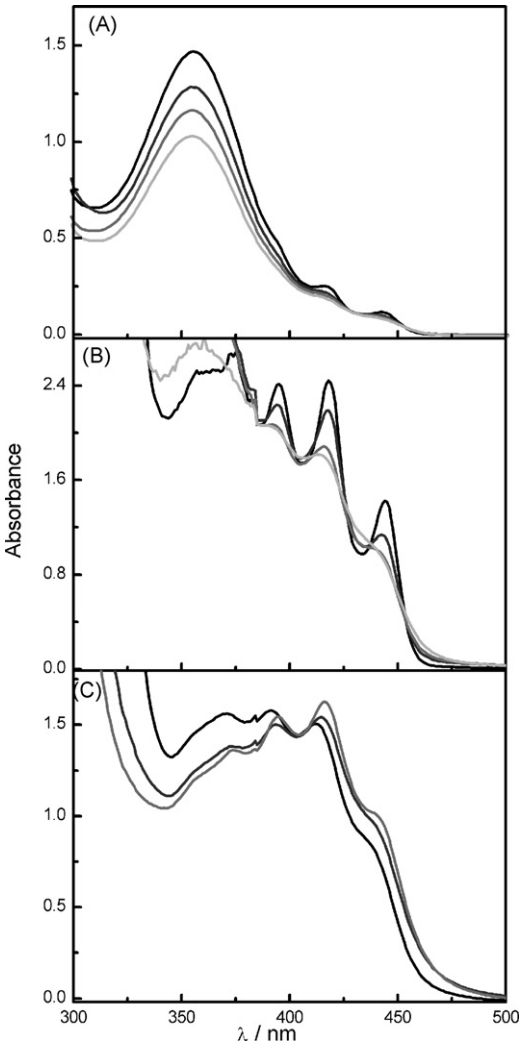

Fig. 3. Electronic absorption spectra obtained upon photolysis of a system comprising an N_2-saturated solution of dye **4** (0.1 mM) and **Py1** (1.0 mM), all dissolved in 1-methyl-2-pyrrolidone. Spectra collected before and after photolysis. Spectra were collected from sample diluted with 1-methyl-2-pyrrolidone (1:1, v/v) (A) and without dilution (B and C).

The free energy change for the photoinduced electron transfer process from excited fluoflavin dyes to the pyridinium salt employed in this study can be calculated from the Rehm–Weller equation (Eq. (5)) [22]:

$$\Delta G_{et}(\text{kJ mol}^{-1}) = 97[E_{ox}(S/S^{\bullet+}) - E_{red}(Py^{\bullet-}/Py)] - Ze^2/\varepsilon a - E^*(S) \quad (5)$$

In this equation, E_{ox} $(S/S^{\bullet+})$ and $E^*(S)$ are, respectively, the oxidation potential and the excited state energy of the fluoflavin dye (electron donor), both of which are shown in Table 2. The reduction potentials E_{red} $(Py^{\bullet-}/Py)$ of the pyridinium salts were measured in the separate experiments and they are presented in Table 3. In this calculation the Coulombic energy $Ze^2/\varepsilon a$ was omitted because the fluoflavin/pyridinium system is the photoredox pair without electrostatic interaction in the ground state and after electron transfer. The calculated thermodynamic parameters listed in Table 3 indicate that all combinations of dye/pyridinium systems possess a high driving force upon exposure to light ($-\Delta G_{et} > 120\,\text{kJ mol}^{-1}$). This means that their photoelectron transfer easily occurs via the excited state. On the basis of these calculations, it can be assumed that the photoinduced intermolecular electron transfer from dyes

Table 3
Characteristics of fluoflavin/Py photoredox pairs

	Py1 ($E^{red}_{1/2} = -1.025$ V)						**Py2** ($E^{red}_{1/2} = -1.225$ V)				
	ΔG^a (kJ mol^{-1})	$K_{SV}{}^b$ (M^{-1})	k_q ($\times 10^{-10}$ M^{-1} s^{-1})	$v^{rel\ c}_{dec}$	Φbl^d ($\times 10^2$ mol quant^{-1})	$\Phi(H^+)^e$ ($\times 10^2$ mol quant^{-1})	ΔG^a (kJ mol^{-1})	$K_{SV}{}^b$ (M^{-1})	k_q ($\times 10^{-10}$ M^{-1} s^{-1})	Φbl^d ($\times 10^2$ mol quant^{-1})	$\Phi(H^+)^f$ ($\times 10^2$ mol quant^{-1})
1	−147.6	53.0	1.25	1.00	1.33	1.70	−128.2	45.5	1.09	0.38	4.67
2	−141.6	56.2	1.70	2.25	3.88	14.20	−122.2	66.8	2.02	2.07	76.00
3	−141.9	50.2	1.42	1.95	1.97	7.10	−122.5	46.2	1.31	1.34	36.00
4	−148.4	54.4	1.30	1.32	1.33	1.50	−129.0	27.6	0.66	0.38	6.10
5	−149.4	232.2	5.63	1.08	1.36	1.70	−130.0	98.6	2.40	0.58	3.00

[a] Free energy change for the electron transfer from singlet excited state of dye.
[b] Stern–Volmer constant for quenching of dye fluorescence by Py in aerated solution.
[c] Relative rate of sensitised photodecomposition of **Py1**: [**Py1**] = 1 mM; [dye] = 0.1 mM.
[d] Quantum yield of dye photobleaching; [Py] = 1 mM; [dye] = 0.1 mM; determined for 14 ± 3%.
[e] Quantum yield of acid release: [Py] = 1 mM; [dye] = 0.1 mM; [BrPhBlue] = 20 μM; determined for 4 ± 1%.
[f] Quantum yield of acid release; [Py] = 1 mM; [dye] = 0.1 mM; [BrPhBlue] = 20 μM; determined for 12 ± 2%.

to pyridinium salts initiates the **Py1** photodecomposition caused by the dyes in this study. The fluorescence of fluoflavin dyes was effectively quenched by pyridinium salt (see inset in Fig. 1), and the absence of any new peak in the emission spectra excludes the exciplex formation. The measured Stern–Volmer constants (K_{SV}) and calculated singlet quenching constants (k_q) are summarised in Table 3. The k_q values are close to the diffusion-controlled limit ($k_q \sim 1 \times 10^{10}\ M^{-1}\ s^{-1}$). Dye **5** has the highest value of k_q, which also has the lowest oxidation potential. This suggests that fluorescent quenching proceeds via electron transfer.

Heavy atoms such as Br in the system are known to promote the formation of the triplet state of the molecule because of the efficient intersystem crossing. In order to clarify the photochemistry of dyes **1**–**5**, their quantum yields of singlet oxygen generation [$\Phi(^1O_2)$] in oxygen-saturated solution were measured (Table 2). The presence of heavy atoms in dyes **2** and **3** explains the increase in the quantum yield of singlet oxygen generation. These two dyes are also the most effective sensitizers for **Py1** decomposition. The relationship between $\Phi(^1O_2)$ and v_{dec}^{rel} suggests that in the case of dyes **2** and **3**, electron transfer may also occur via the triplet state [3,4].

3.3. Dye photobleaching

In the photopolymerization of multifunctional monomers initiated by a dye photoredox pair, the most important properties are high initiation reactivity and photobleaching of the dye. The photobleaching of dyes **1**–**5** was measured in 1-methyl-2-pyrrolidone solution under an N_2 atmosphere. The photobleaching quantum yields of the dyes (Φbl) are presented in Table 3. These data clearly indicate that dyes **2** and **3** show the highest photobleaching quantum yield and these compounds are the most promising photosensitizers for VIS curing.

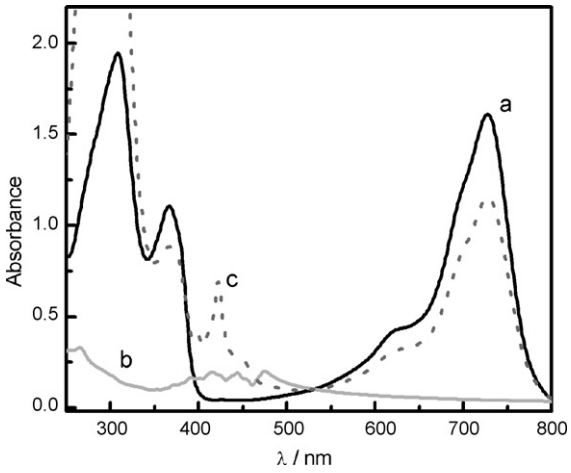

Fig. 4. Electronic absorption spectra of Magic Blue (curve a), dye **5** (b) and the solution obtained by adding of dye **5** to a solution of Magic Blue in CH_2Cl_2 (c).

The absorption spectra of the combination of fluoflavin dye **4** and pyridinium salt **Py1** before and during irradiation for 10–30 s are shown in Fig. 3B. Decay of the dye absorption (at 396 nm, 415 nm, and 440 nm) is accompanied by the growth of the bands at ~360 nm and ~465 nm. The same effect was observed during photolysis of the dye/**Py2** system. The isosbestic points (Fig. 3) indicate direct conversion of the dye to the product, which is very stable. Extending the irradiation time to 120–600 s increased the absorption in the range of 400–475 nm and caused it to red-shift. In order to explain this effect, the product of one-electron oxidation of dye **5** was characterized spectrophotometrically. Fig. 4 presents the absorption spectra of the mixture of fluoflavin dye **5** (15 μM, curve b) with

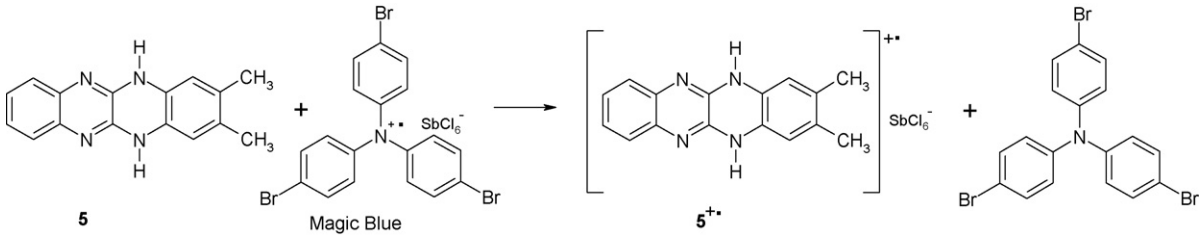

Scheme 5.

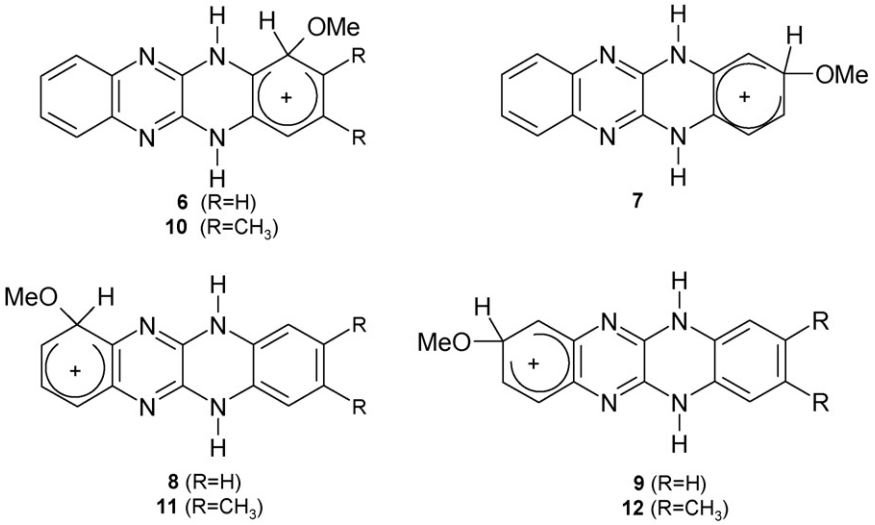

Scheme 6.

Table 4
Relative energies of the cation (kJ mol^{-1}, relative to the most stable form) and the gas phase acidity of the cations **9** and **10**

Dye	Cation				ΔE_{elec}[a]	$\Delta E(0)$[b]	$\Delta E(298)$[c]	$\Delta H(298)$[d]
	6	**7**	**8**	**9**				
1	6.69	5.45	4.62	0	889.6	858.3	830.6	833.1
	10		**11**	**12**				
5	11.36	–	6.47	0	903.4	872.1	844.0	846.5

[a] $\Delta E_{elec} = E(\text{DyeOMe}) - E(\text{HDyeOMe}^+)$.
[b] $\Delta E(0) = \Delta E_{elec} + \Delta ZPE$, where ZPE is the zero-potential energy correction.
[c] $\Delta E(298) = \Delta E(0) + \Delta E(0–298) + 3RT/2$, where $\Delta E(0–298)$ is the thermal correction from 0 to 298 K and $3RT/2$ corresponds to the translation energy of the proton.
[d] $\Delta H(298) = \Delta E(298) + RT$, where RT is the pV-contribution due to one extra mol of gas after deprotonation.

Magic Blue [23] (50 μM, curve a). The decay of the Magic Blue absorption at 728 nm is accompanied by the appearance of a new absorption band in the range of 420–450 nm (curve c). The reaction takes place in the stoichiometry of 1 mol Magic Blue:1 mol dye, which may indicate formation of the cation radical **5**$^{\bullet+}$ (Scheme 5). The absorption band of **5**$^{\bullet+}$ is blue-shifted relative to the absorption of the parent dye in CH_2Cl_2 (curve b). This rules out the possibility that the cation radical is responsible for the increased absorption of the dye/pyridinium system during photolysis.

Similarly, the formation of a new product, with an absorption peak red-shifted relative to that of the sensitizer, was observed during photodecomposition of anthracene-sensitised Ph_2IPF_6 [24] and **Py2** [25]. Mechanisms were proposed for these systems involving reaction between the anthracene cation radical and the phenyl or ethoxyl radical, respectively.

In the present study the formation of the cation **1-OMe**$^+$ and **5-OMe**$^+$ in the irradiated fluoflavin/pyridinium system was estimated on the basis of quantum chemical calculations for symmetrical dyes **1** and **5**. Since the reaction between the cation radical of the dye and the alkoxy radical can produce four different cationic species (Scheme 6), DFT calculations at the B3LYP/6-31G* level were carried out to compare the relative stabilities of the possible structures (cations **6**–**12**). Considering the high relative energy (4.62–11.36 kJ mol^{-1}, Table 4) of the cations **6**–**8** relative to the cation **9**, and cations **10**, **11** relative to the cation **12**, it seems that most stable form for dyes **1** and **5** in the gas phase are the cations **9** and **12**, respectively. Therefore, one can assume that the radical cation of the fluoflavin dye reacts with the alkoxy radical at the phenyl ring at position 9. Moreover, deprotonation energies (acidities) define as the difference in calculated energy between methoxy derivative of dyes **1-OMe**/**5-OMe** and cations **9**/**12** were calculated and the results are given in Table 4. The relative gas phase acidity [$\Delta H(298)$] of **9** and **12** is high [26], so these cations should undergo deprotonation to alkoxy dyes **1-OMe** and **5-OMe**, respectively, which may be responsible for the increase in absorption in the range of 400–475 nm.

In order to confirm the above calculations, the quantum yield of acid release [$\Phi(H^+)$] in the solution upon photolysis was measured using sodium bromophenol blue (**BPhBl**, Scheme 7), the absorption of which at the peak wavelength at 606 nm decreased during irradiation (Fig. 5). The amount of acid release was estimated from the calibration curve of **BPhBl** (inset in Fig. 5). In all the dye/pyridinium combinations studied the solution acidity increased, whereas photolysis of the dyes alone left the solution pH unchanged.

The calculated quantum yields of acid release are presented in Table 3. Dyes **2** and **3** showed the highest quantum yield of acid release. Moreover, in all cases the quantum yield of acid release was higher then the photobleaching quantum yield. These results suggest that photolysis of fluoflavin dye/Py systems produces a new methoxy or ethoxy fluoflavin dye. Moreover, after photolysis of solution **5** and **Py1**, two fluorescent products were detected by TLC chromatography. These new dyes show an absorption band in the same wavelength as the parent dye.

On the basis of the results presented above, Scheme 8 proposes a mechanism for how photobleaching of fluoflavin dyes composed of pyridinium salts occurs during photolysis. Scheme 8 takes as its example the system of dye **1** and **Py2**. Electron transfer proceeds from the excited dye to the pyridinium salt (**Py2**), followed by cleavage of the ethoxypiridinium radical (**Py2**$^\bullet$) to give ethoxy radical ($^\bullet$OEt), neutral pyridine, and dye radical cation (**1**$^{\bullet+}$). The fluoflavin cation radical may react with ethoxy radical ($^\bullet$OEt) yielding cation **9**, followed by proton release and formation of an ethoxy derivative of fluoflavin dye **1-OEt**.

3.4. Photopolymerization

Finally, the fluoflavin-sensitised Py photodecomposition system was examined for its usefulness as the initiator for free radical poly-

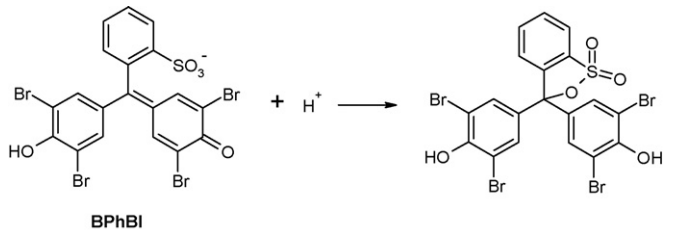

Scheme 7.

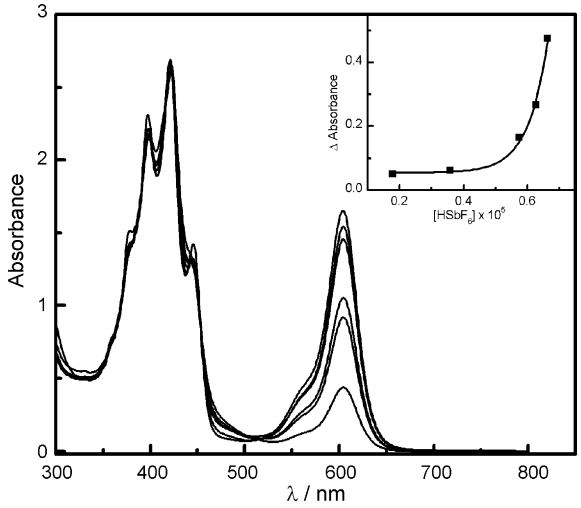

Fig. 5. Electronic absorption spectra obtained upon photolysis (time interval, 15 s) of an N_2-saturated solution **BPhBl** (20 μM) and a dye **5** (0.1 mM)/**Py2** (1.0 mM) system in 1-methyl-2-pyrrolidone. *Inset*: calibration curve of **BPhBl** (20 μM) vs. $HSbF_6$ concentration (range 0–70 μM).

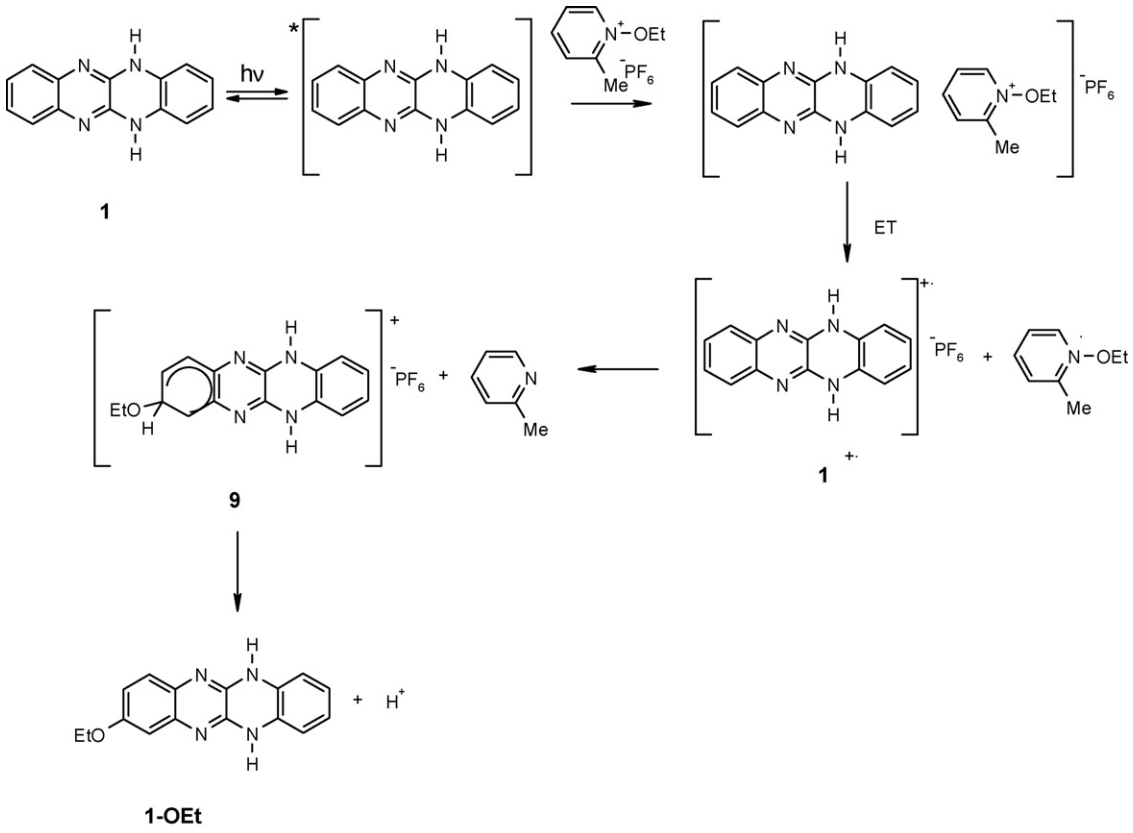

Scheme 8.

merization of a methyl acrylate (MeAc) and trimethylolpropane triacrylate monomer. The efficiency of the polymerization initiated by fluoflavin/Py systems was assessed from the heat flow during the irradiation (Fig. 6A and B). In the case of MeAc the conversion of the monomer into polymer was also determined after the irradiation. These results are summarised in Table 5.

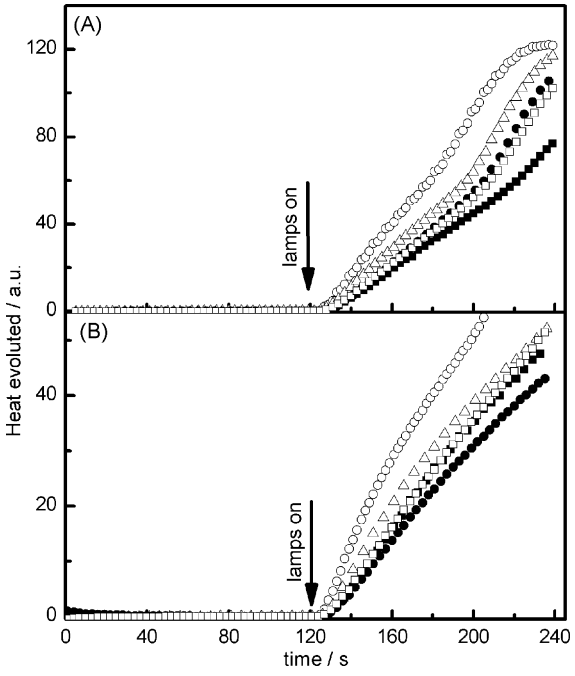

Fig. 6. Photopolymerization kinetic curves of TMPTA recorded for dyes **1** (■); **2** (○); **3** (▲); **4** (●); **5** (□) and (A) **Py1** or (B) **Py2**.

Table 5
Rate of photopolymerization (μmol s^{-1}) and conversion (%) of the monomer in the polymerization initiated by the fluoflavin/Py system

	Py1			Py2		
	TMPTA	MeAc		TMPTA	MeAc	
	Rp	Rp	%	Rp	Rp	%
1	18.8	12.3	11	11.7	12.9	8
2	29.4	17.8	15	25.1	20.9	15
3	28.3	14.5	11	12.5	16.7	13
4	26.2	12.2	9	10.4	15.2	10
5	25.0	12.5	10	12.5	16.7	10

Fig. 6 and the calculated polymerization rate (Table 5) indicate that the efficiency of polymerization strongly depends on the type of electron donor and on the structure of the dye. It is apparent that the fluoflavin dye **2** significantly accelerates the photopolymerization of acrylate and triacrylate monomer. Moreover, **Py1** is a more effective initiator than **Py2**.

4. Conclusions

Fluoflavin dyes sensitize *N*-alkoxypyridinium salts to photodecomposition. Sensitization occurs through electron transfer. In the decomposition of a sensitised alkoxypyridinium salt, the proton is released from the cation (**Dye-OR$^+$**), which is formed in the reaction of the fluoflavin cation radical and the alkoxy radical. These photodecomposition systems may have practically applications as photoinitiators of free radical polymerization of acrylate monomers in visible light.

Acknowledgements

This work was supported by the Polish Ministry of Science and Higher Education (Project no. N N205 1454 33).

References

[1] C. Lowe, G. Webster, S. Kessel, I. McDonald, Chemistry and technology of UV and EB formulation for coatings, inks and paints Surface Coating Technology, vol. 4, Wiley, London, 1996;
P.K.T. Oldring, Chemistry and technology of UV and EB formulation for coatings, inks and paints Speciality Finishes, vol. 5, Wiley–Sita Techn. Ltd., London, 1997;
J. Jakubiak, J.F. Rabek, Polimery 45 (2000) 759–770.
[2] N.S. Allen, J. Photochem. Photobiol. A: Chem. 100 (1996) 101–109.
[3] Z. Kucybała, J. Pączkowski, J. Photochem. Photobiol. A: Chem. 128 (1999) 135–138.
[4] B. Przyjazna, Z. Kucybała, J. Pączkowski, Polymer 45 (2004) 2559–2566.
[5] S. Chatterjee, P. Gottschalk, P.D. Davis, G.B. Schuster, J. Am. Chem. Soc. 110 (1988) 2326–2328;
S. Chatterjee, P.D. Davis, P. Gottschalk, P. Kurz, X. Yang, G.B. Schuster, J. Am. Chem. Soc. 112 (1990) 6329–6338.
[6] I.R. Gould, D. Shukla, D. Giesen, S. Farid, Helv. Chim. Acta 84 (2001) 2796–2812.
[7] H.J. Timpe, K.P. Kronfeld, U. Lannel, J.P. Fouassier, D.J. Lougnot, J. Photochem. Photobiol. A: Chem. 52 (1990) 111–122.
[8] H.J. Timpe, S. Urlich, J.P. Fouassier, Macromolecules 26 (1993) 4560–4566.
[9] J.P. Fouassier, X. Allonas, D. Burget, Prog. Org. Coat. 47 (2003) 16–36.
[10] S. Hunig, D. Scheutzow, H. Schlaf, H. Quast, Liebigs Ann. Chem. 765 (1972) 110–125.
[11] C. Reichardt, Chem. Ber. 97 (1966) 1769–1770.
[12] W.B. Leighton, G.S. Forbes, J. Am. Chem. Soc. 52 (1930) 3139–3152.
[13] S.C. Nunez Montoya, L.R. Comini, M. Sarmiento, C. Becerra, I. Albesa, G.A. Argüello, J.L. Cabrera, J. Photochem. Photobiol. B: Biol. 78 (2005) 77–83.
[14] T. Karstens, K. Kobs, J. Phys. Chem. 84 (1980) 1871–1872.
[15] D. Avci, J. Nobles, L.J. Mathias, Polymer 44 (2003) 963–968.
[16] J.F. Coetzee, J.J. Campion, J. Am. Chem. Soc. 89 (1967) 2513–2517.
[17] A.D. Becke, J. Chem. Phys. 98 (1993) 5648–5652.
[18] C. Lee, W. Yang, R.G. Parr, Phys. Rev. B 37 (1988) 785–789.
[19] M.J. Frisch, G.W. Trucks, H.B. Schlegel, G.E. Scuseria, M.A. Robb, J.R. Cheeseman, V.G. Zakrzewski, J.A. Montgomery, R.E. Stratmann, J.C. Burant, S. Dapprich, J.M. Millam, A.D. Daniels, K.N. Kudin, M.C. Strain, O. Farkas, J. Tomasi, V. Barone, M. Cossi, R. Cammi, B. Mennucci, C. Pommelli, C. Adamo, S. Clifford, J. Ochterski, G.A. Petersson, P.Y. Ayala, Q. Cui, K. Morokuma, D.K. Malick, A.D. Rabuck, K. Raghavachari, J.B. Foresman, J. Cioslowski, J.V. Ortiz, B.B. Stefanov, G. Liu, A. Liashenko, P. Piskorz, I. Komaromi, R. Gomperts, R.L. Martin, D.J. Fox, T. Keith, M.A. Al-Laham, C.Y. Peng, A. Nanayakkara, M. Challacombe, P.M.W. Gill, B.G. Johnson, W. Chen, M.W. Wong, J.L. Andres, C. Gonzales, M. Head-Gordon, E.S. Repogle, J.A. Pople, Gaussian 98, Rev. A9, Gaussian, Inc., Pittsburgh, PA, 1998.
[20] G. Kaup, M.R. Naimi-Jamal, Eur. J. Org. Chem. (2002) 1368–1373.
[21] G. Riedel, W. Deuschel, patent GB 971048.
[22] D. Rehm, A. Weller, Isr. J. Chem. 8 (1970) 259–271.
[23] N.G. Connelly, W.E. Geiger, Chem. Rev. 96 (1996) 877–910.
[24] H. Kura, K. Fujihara, A. Kimura, T. Ohno, M. Matsumura, Y. Hirata, T. Okada, J. Polym. Sci. B: Polym. Phys. 39 (2001) 2937–2946.
[25] D. Dossow, Q.Q. Zhu, G. Hizal, Y. Yagci, W. Schnabel, Polymer 37 (1996) 2821–2826.
[26] F. Bökman, J. Am. Chem. Soc. 121 (1999) 11217–11222.